Stereoselective 1,3-Dipolar Cycloadditions of a Chiral Nitrone Derived from Erythrulose. An Experimental and DFT Theoretical Study

Miguel Carda,[†] Raul Portolés,[†] Juan Murga,[†] Santiago Uriel,[†] J. Alberto Marco,[‡,*] Luis R. Domingo,[‡,*] Ramón J. Zaragozá,[‡] and Harald Röper[§]

U. P. de Química Inorgánica y Orgánica, Universidad Jaume I, E-12080 Castellón, Spain; Departamento de Química Orgánica, Universidad de Valencia, E-46100 Burjassot, Valencia, Spain; and Eridania Béghin-Say, R&D Centre, Havenstraat 84, B-1800 Vilvoorde, Belgium

alberto.marco@uv.es

Received June 26, 2000

We have investigated several 1,3-dipolar cycloadditions of a chiral nitrone prepared from L-erythrulose. While cycloadditions to carbon−carbon multiple bonds of dipolarophiles such as ethyl acrylate, ethyl propiolate, or dimethyl acetylenedicarboxylate were poorly stereoselective, reaction with acrylonitrile provided predominantly one diastereomeric adduct. Furthermore, the regioselectivity exhibited by the two structurally similar dipolarophiles ethyl acrylate and ethyl propiolate was found to be opposite. The molecular mechanisms of these cycloadditions have thus been investigated by means of density functional theory (DFT) methods with the B3LYP functional and the 6-31G* and 6-31+G* basis sets. A simplified achiral version of nitrone **1** as the dipole, and methyl propiolate or acrylonitrile as the dipolarophiles, were chosen as computational models. The cycloadditions have been shown to take place through one-step pathways in which the C−C and C−O σ bonds are formed in a nonsynchronous way. For the reaction with methyl propiolate, DFT calculations predict the experimentally observed *meta* regioselectivity. For the reaction with acrylonitrile, however, the predicted regioselectivity has been found to depend on the computational level used. The calculations further indicate the *exo* approach to be energetically favored in the case of the latter dipolarophile, in agreement with experimental findings. The main reason for this is the steric repulsion between the nitrile function and one of the methyl groups on the nitrone that progressively develops in the alternative *endo* approach.

Introduction

Nitrones are compounds with a broad synthetic potential. The highly polar C═N bond, for instance, is appreciably reactive toward the addition of many types of nucleophilic reagents.[1] In such reactions, a new C−C bond is created with the formation of substituted N-hydroxy amines. After reductive cleavage of the N−O bond in the latter, many types of nitrogenated compounds such as *sec*- and *tert*-alkylamines, amino acids, amino alcohols, amino sugars, etc., can be made available through suitable synthetic manipulations. In addition, nitrones are able to undergo 1,3-dipolar cycloadditions (1,3-DCs) to various types of multiple bonds, most usually C═C or C≡C bonds.[2−4] In this case, a new C−C bond is created and either dihydro or tetrahydro isoxazoles are formed. Here again, reductive cleavage of the N−O bond opens the way to further types of nitrogenated compounds (Scheme 1).

As part of our research on the synthesis of enantiopure nonproteinogenic amino acids, most particularly α,α-disubstituted α-amino acids,[5] we have recently reported on the stereoselective additions of various organometallics to the C═N bond of the chiral, erythrulose-derived nitrone **1**,[6] prepared as depicted in Scheme 2. As a potentially useful alternative to this reaction type, we have considered the formation of a C−C bond via 1,3-DCs of **1** to olefins (Scheme 3). Should this process display a sufficiently high degree of stereoselectivity, this would

* To whom correspondence should be addressed: J. Alberto Marco (experimental aspects) or Luis R. Domingo (theoretical questions). Phone no.: 34-96-3864337. Fax no.: 34-96-3864328. e-mail (L.R.D.): domingo@utopia.uv.es.

[†] Universidad Juame I.

[‡] Universidad de Valencia.

[§] Eridania Béghin-Say.

(1) Bloch, R. *Chem. Rev.* **1998**, *98*, 1407−1438. See also: Adams, J. P.; Box, D. S. *J. Chem. Soc., Perkin Trans. 1* **1999**, 749−764.

(2) For two recent reviews with numerous references to previous literature, see: (a) Frederickson, M. *Tetrahedron* **1997**, *53*, 403−425. (b) Gothelf, K. V.; Jørgensen, K. A., *Chem. Rev.* **1998**, *98*, 863−909.

(3) For recent examples of intermolecular nitrone-olefin cycloadditions, see: (a) Xu, Z.; Johannes, C. W.; La, D. S.; Hofilena, G. E.; Hoveyda, A. H. *Tetrahedron* **1997**, *53*, 16377−16390. (b) Closa, M.; de March, P.; Figueredo, M.; Font, J.; Soria, A. *Tetrahedron* **1997**, *53*, 16803−16816. (c) Kobayashi, S.; Kawamura, M. *J. Am. Chem. Soc.* **1998**, *120*, 5840−5841. (d) Aggarwal, V. K.; Grainger, R. S.; Adams, H.; Spargo, P. L. *J. Org. Chem.* **1998**, *63*, 3481−3485. (e) Gothelf, K. V.; Hazell, R. G.; Jørgensen, K. A. *J. Org. Chem.* **1998**, *63*, 5483−5488. (f) Borrachero, P.; Cabrera, F.; Diánez, M. J.; Estrada, M. D.; Gómez-Guillén, M.; López-Castro, A.; Moreno, J. M.; de Paz, J. L.; Pérez-Garrido, S. *Tetrahedron: Asymmetry* **1999**, *10*, 77−98. (g) Simonsen, K. B.; Bayón, P.; Hazell, R. G.; Gothelf, K. V.; Jørgensen, K. A. *J. Am Chem. Soc.* **1999**, *121*, 3845−3853.

(4) For recent examples of intramolecular cycloadditions of unsaturated nitrones, see: (a) Bar, N. C.; Roy, A.; Achari, B.; Mandal, S. B. *J. Org. Chem.* **1997**, *62*, 8948−8951. (b) Arnone, A.; Broggini, G.; Passarella, D.; Terraneo, A.; Zecchi, G. *J. Org. Chem.* **1998**, *63*, 9279−9284.

(5) (a) Marco, J. A.; Carda, M.; Murga, J.; Rodríguez, S.; Falomir, E.; Oliva, M. *Tetrahedron: Asymmetry* **1998**, *9*, 1679−1701. (b) Carda, M.; Murga, J.; Rodríguez, S.; González, F.; Castillo, E.; Marco, J. A. *Tetrahedron: Asymmetry* **1998**, *9*, 1703−1712.

(6) Marco, J. A.; Carda, M.; Murga, J.; Portolés, R.; Falomir, E.; Lex, J. *Tetrahedron Lett.* **1998**, 3237−3240.

10.1021/jo0009651 CCC: $19.00
Published on Web 09/22/2000

Scheme 1

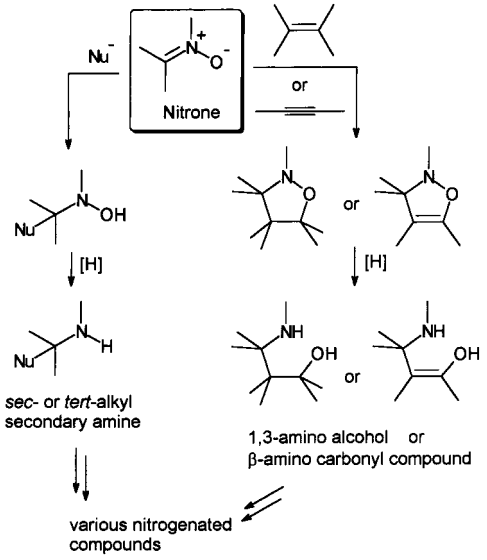

Scheme 2

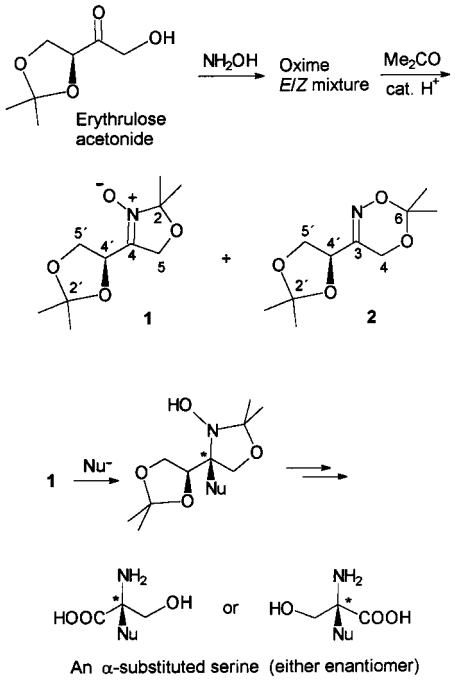

Scheme 3

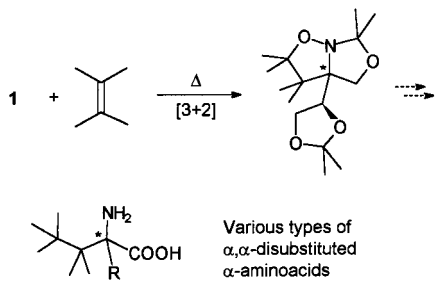

be another useful approach to chiral, nitrogen-containing adducts which, after the requisite manipulation, should then be amenable to conversion into various types of α,α-disubstituted α-amino acids.

When nitrones and other unsymmetrical 1,3-dipoles are allowed to react with multiple carbon−carbon bonds of either olefins or acetylenes, issues of both regioselectivity and stereoselectivity are of concern. To delimit these two aspects in the particular case of nitrone **1**, we have investigated its 1,3-DCs to several dipolarophiles. Since a mechanistic interpretation of the observed results, both in terms of regioselectivity and stereoselectivity, was not possible by relying on simple qualitative considerations, we have performed ab initio studies on some of these reactions. The discussion of these experimental and theoretical findings is the object of the present paper.

In contrast to the Diels−Alder reaction, which has received a great deal of theoretical attention,[7] there are not many computational studies of 1,3-DCs of nitrones to multiple carbon−carbon bonds.[8] In one study, Tanaka et al.[8a] used semiempirical methods to examine the 1,3-DC of a 3,4-dihydroisoquinoline to methyl 2-butenoate. These authors proposed a concerted mechanism with a nonsymmetric transition structure (TS) in which the C−O bond is formed to a greater degree than the C−C bond. The exclusive formation of the *endo* adduct was attributed to the stabilizing secondary orbital interactions of the ester carbonyl group with both the phenyl ring and the HOMO lobe on the nitrogen atom. More recently, Houk et al.[8c] have performed ab initio calculations at the B3LYP/6-31G* level on the 1,3-DC of the simple unsubstituted nitrone (UN, $CH_2{=}N^+H{-}O^-$) to dipolarophiles containing electron-releasing substituents. Here again, the *endo* approach is kinetically favored because of stabilizing secondary orbital interactions.

The regioselectivity of these 1,3-DCs has been recently studied by Magnuson and Pranata using ab initio methods (B3LYP/6-31G*).[8e] While in the 1,3-DCs between UN and electron-rich alkenes (e.g., aminoethylene), the *ortho* regioisomers are predicted to be formed in a higher proportion than the *meta* regioisomers (see Scheme 6 for these regiochemical descriptors), calculations predict that the reactions with electron-poor alkenes such as acrylonitrile will be nonregioselective; UN exhibits a preferred *endo* selectivity because of stabilizing secondary orbital interactions. Recently, Cossío et al.[8f] have used B3LYP/6-31+G* calculations to study the 1,3-DC of UN with nitroethylene. The asynchronicity in the bond formation process in the two regioisomeric approaches of nitroethene to the nitrone is controlled by the electron-poor dipolarophile; the forming bond at the β-position of nitroethylene is shorter than that at the α-position. Their calculations predict an *endo* stereoselectivity, but the predicted *meta* regioselectivity does not agree with experimental findings. These authors suggest that the regioselectivity of these reactions cannot be predicted by means of simple electronic arguments. Steric and polar effects, including those due to the solvent, must be taken into consideration to account for both the regio- and the stereochemical outcome.[8f]

One of us has recently studied the 1,3-DC of *N*-benzylidene aniline *N*-oxide to the electron-rich olefin

(7) (a) Sauer, J.; Sustmann, R. *Angew. Chem., Int. Ed. Engl.* **1980**, *19*, 778−807. (b) Houk, K. N.; González, J.; Li, Y. *Acc. Chem. Res.* **1995**, *28*, 81−90.

(8) (a) Tanaka, K.; Imase, T.; Iwata, S. *Bull. Chem. Soc. Jpn.* **1996**, *69*, 2243−2248. (b) Raimondi, L. *Gazz. Chim. Ital.* **1997**, *127*, 167−175. (c) Liu, J.; Niwayama, S.; You, Y.; Houk, K. N. *J. Org. Chem.* **1998**, *63*, 1064−1073. (d) Yeung, M. L.; Li, W. K.; Liu, H. J.; Wang, Y.; Chan, K. S. *J. Org. Chem.* **1998**, *63*, 7670−7673. (e) Magnuson, E. C.; Pranata, J. *J. Comput. Chem.* **1998**, *19*, 1795−1804. (f) Cossío, F. P.; Morao, I.; Jiao, H.; Schleyer, P. von R. *J. Am. Chem. Soc.* **1999**, *121*, 6737−6746. (g) Domingo, L. R. *Eur. J. Org. Chem.* **2000**, 2273−2284.

Scheme 4

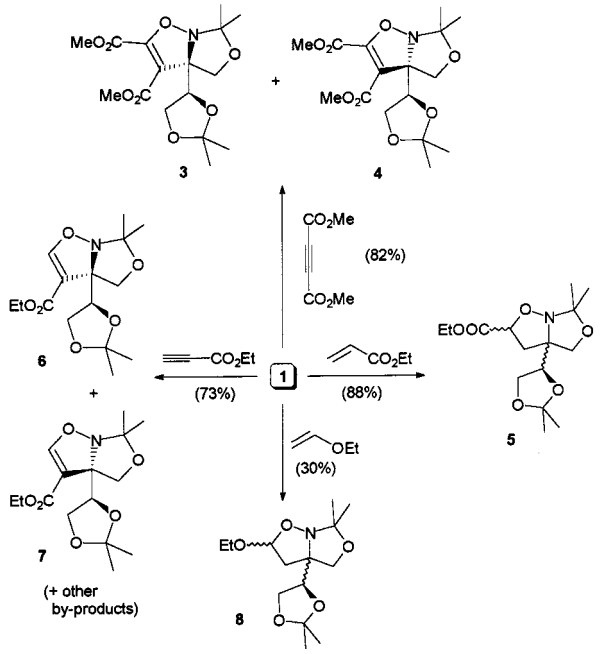

Scheme 5

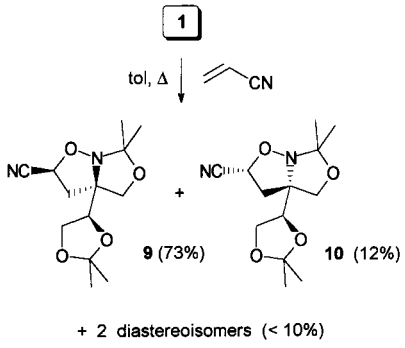

Scheme 6

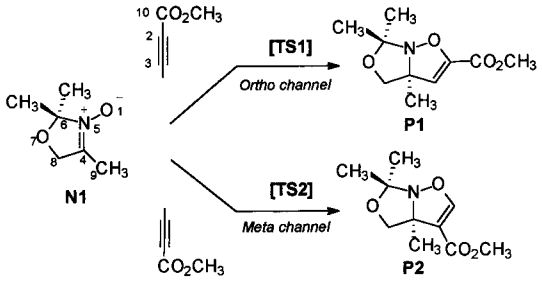

tert-butyl vinyl ether.[8g] B3LYP/6-31G* calculations predict an *exo* stereoselectivity together with an *ortho* regioselectivity in agreement with experimental findings.[3g] The *exo* selectivity is due to a steric hindrance that progressively develops along the *endo* approach between a phenyl group on the N atom and the *tert*-butyl group of the vinyl ether. Inclusion of solvent effects increases the activation energies and decreases the exothermic character of the process because of a greater solvation of the polar nitrone than that of the TSs and cycloadducts.[8f,g] Solvents also cause a higher stabilization of the *endo* TS and therefore a slight decrease in the stereoselectivity.

These studies indicate that the predicted regio- and stereochemical results depend on the computational model. As a matter of fact, the *endo* stereoselectivity predicted for the structurally simple UN is not in agreement with experimental findings for more complex nitrones. These results suggest the necessity of using more realistic models and much higher computational levels in order to reproduce the chemical outcome of these 1,3-DCs.

Table 1. 1, 3-Dipolar Cycloadditions of Nitrone 1 to Dipolarophiles[a]

Dipolarophile	Yield (%)	Diastereomeric ratio[b]
$MeO_2C{-}{\equiv}{-}CO_2Me$	82	60 : 40
$\equiv CO_2Et$	73	65 : 35
CO_2Et	88	41 : 34 : 17 : 8
OEt	30[c]	75 : 25
CN	95	77 : 13 : 5 : 5

[a] The reagents were heated at reflux in toluene for 2 h (see Experimental Section). [b] Determined by ^1H and ^{13}C NMR. [c] The reaction was performed under pressure in a closed system with the dipolarophile as the solvent.

Results and Discussion

1. Cycloaddition Reactions and Stereochemical Assignments. As mentioned above, 1,3-DCs may present both regioselectivity and stereoselectivity issues. To investigate both aspects separately, we first heated a mixture of **1** and dimethyl acetylenedicarboxylate which, due to its symmetry and acetylenic nature, could only give rise to two stereoisomeric cycloadducts. The reaction did not prove useful from the preparative point of view, as both stereoisomers, **3** and **4**, were formed in a similar proportion (see Scheme 4 and Table 1). Their structures were established via an X-ray diffraction analysis of the major cycloadduct **3**.[9] We then turned our attention to other dipolarophiles, both electron-poor, such as ethyl acrylate, ethyl propiolate, and acrylonitrile, and electron-rich olefins, such as cyclohexene, 2,3-dimethyl-2-butene, and ethyl vinyl ether. With ethyl acrylate, the reaction was completely regioselective and only cycloadducts of gross structure **5** (Scheme 4) were formed.[10] Unfortunately, the reaction displayed a low stereoselectivity and yielded all four possible stereoisomers in a ca. 5:4:2:1 ratio. In view of the lack of synthetic utility of this

(9) Crystallographic data of compounds **3**, **6**, **9**, and **10** have been deposited in the Cambridge Crystallographic Data Centre, 12 Union Road, Cambridge CB2 1EZ, U.K., and may be requested from the Director of this Centre.

(10) This was deduced from an examination of the methylene signals in the ^{13}C NMR spectrum of the reaction mixture. No new signals from oxygenated methylenes, expected for regioisomers **i**, were found. Instead, four new methylene signals appeared in the range 44−40 ppm, which were only possible for regioisomers **ii** (see arrows in the structures below).

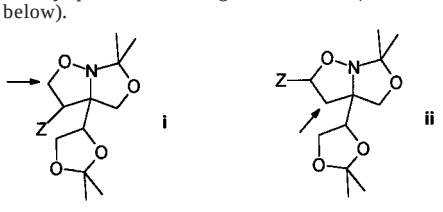

Scheme 7

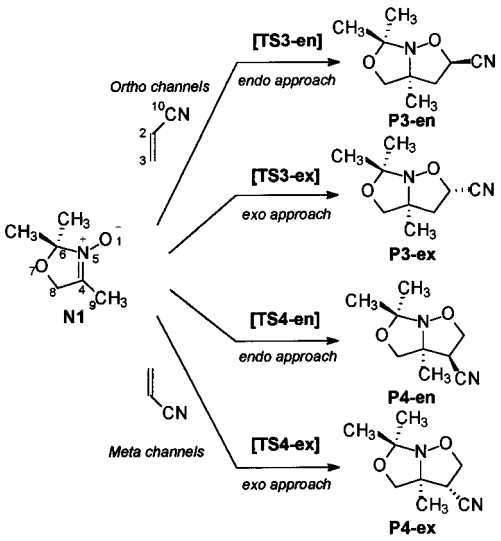

process, the compounds were not isolated. The reaction with ethyl propiolate was also disappointing from the preparative point of view. The reaction displayed a good regioselectivity but a poor stereoselectivity. Two stereoisomers **6** (major) and **7** were formed together with other undefined byproducts.[9] No reaction at all was observed with cyclohexene or 2,3-dimethyl-2-butene, even after 18 h at 150 °C under pressure in a closed system. Under the same conditions, ethyl vinyl ether gave a mixture of two diastereomers with gross structure **8** in a low overall yield (30%). As in the case of **5**, the stereoisomers were not isolated.

With acrylonitrile, we were pleased to find a synthetically useful process. When the reaction was conducted at reflux in toluene, two cycloadducts, **9** and **10** (Scheme 5), were isolated in 73 and 12% yield, respectively, by means of column chromatography. Their structures were established with the aid of X-ray diffraction studies.[9] No other compounds were isolated in a pure state from the chromatographic column, but an NMR examination of the crude reaction mixture revealed that the cycloaddition was totally regioselective, with the nitrone oxygen bonded exclusively to the nitrile-bearing carbon.[10] All four possible stereoisomeric adducts were formed but the two minor adducts (less than 10% overall as estimated by means of NMR) were not isolated.

To account for the aforementioned experimental results, a theoretical study of some of these 1,3-DCs has been carried out (see Experimental Section for details of the computing methods). In 1,3-DCs involving nonsymmetric dipoles, such as **1**, and nonsymmetric olefinic dipolarophiles, such as acrylonitryle or ethyl acrylate, three types of selectivity have to be taken into account: regioselectivity, *endo*/*exo* stereoselectivity, and π-facial stereoselectivity. Consequently, a total of up to eight isomeric cycloadducts may be formed along eight reaction channels. Unfortunately, if the nitrone contains a bulky chiral substituent (as is the case in **1**), which is responsible for the π-facial selectivity of the reaction, the various conformations of the chiral pendant must also be taken into account for the study. At any DFT level, such a theoretical study may become extremely time-consuming. For this reason, a reduced nitrone model **N1** (Schemes 6 and 7) was used in which the chiral acetal moiety of **1** has been replaced by a methyl group. While this reduced

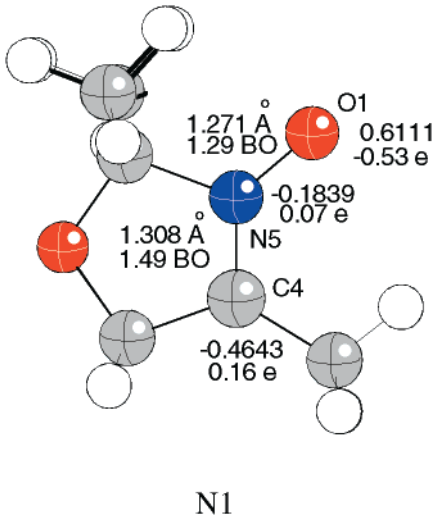

Figure 1. B3LYP/6-31G* optimized geometry of nitrone **N1**. Bond lengths, Wiberg bond orders, natural charges, and HOMO coefficients for the O1, C4, and N5 atoms are included.

model lacks any π-facial selectivity, it makes the study of the regioselectivity and the *endo*/*exo* stereoselectivity of the reaction computationally feasible.

2. Theoretical Study of the Molecular Structure of Nitrone N1. Before proceeding to the study of the molecular mechanism of the aforementioned 1,3-DCs, the geometry of nitrone **N1** was optimized. Figure 1 shows the geometry of **N1**, including several electronic and structural parameters. The O1−N5 and C4−N5 bond lengths are 1.271 and 1.308 Å, respectively. Although the O1−N5 bond turns out to be shorter than the C4−N5 bond, the bond order analysis[11] shows that the former (1.29 BO) has more of a single bond character than the latter (1.49 BO). This geometrical feature is due to the fact that an N−O bond is shorter than an N−C bond. The natural population analysis for this nitrone indicates that the O1 oxygen atom supports a negative charge (−0.5 e), while the C4 carbon atom supports a small positive charge (0.2 e).

When compared with Diels−Alder reactions, 1,3-DCs of nitrones to olefins usually exhibit lower levels of both regioselectivity and stereoselectivity. This is a consequence of the significant contribution of $HOMO_{dipole}$−$LUMO_{dipolarophile}$ as well as $HOMO_{dipolarophile}$−$LUMO_{dipole}$ interactions.[2b,3d] However, the frontier molecular orbital (FMO) analysis for the cycloadditions under study shows that the main interactions occur here between the $HOMO_{dipole}$ of the nitrone (−5.706 eV) and the $LUMO_{dipolarophile}$ of the electron-poor alkenes, either methyl propiolate or acrylonitrile (−1.203 and −1.527 eV, respectively) (Figure 2). These two dipolarophiles have similar FMO energies.

In principle, the regioselectivity could be rationalized in terms of a more favorable FMO interaction between the largest coefficient centers of the dipole and dipolarophile. However, an analysis of the HOMO of **N1** shows that both the O1 oxygen and the C4 carbon display similar molecular coefficient values (0.6 and −0.5, respectively). Furthermore, both dipolarophiles exhibit similar LUMO coefficients at the acetylenic and ethylenic systems. It is thus difficult to predict the regioselectivity

(11) Wiberg, K. B. *Tetrahedron* **1968**, *24*, 1083−1096.

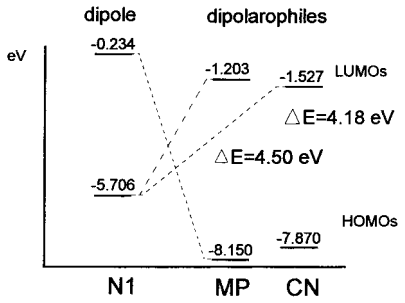

Figure 2. Frontier molecular orbital interactions (B3LYP/6-31G*) in the 1,3-DCs of nitrone **N1** to methyl propiolate (**MP**) or acrylonitrile (**CN**).

of the process, a circumstance which is in agreement with the lower regioselectivity often found for 1,3-DCs, as compared with [4 + 2] cycloadditions.[12]

3. 1,3-DC of N1 to Methyl Propiolate. (a) Energies. To simplify the calculations, methyl propiolate, instead of ethyl propiolate, was taken as the model dipolarophile. Two reaction channels, *ortho* and *meta*, corresponding to the two regioisomeric possibilities of approach of the dipolarophile to dipole **N1** have been considered (Scheme 6). The *ortho* reaction channel corresponds to the O1−C2 and C3−C4 bond-forming processes, whereas the *meta* channel corresponds to the O1−C3 and C2−C4 bond-forming processes. We have thus considered two TSs: **TS1** and **TS2**, which correspond to the approach of the dipolarophile to the dipole along the *ortho* and *meta* pathways, respectively. A schematic representation of the stationary points in the two regioisomeric attacks of methyl propiolate to **N1** is presented in Scheme 6, together with the atom numbering.

The geometries of the TSs are displayed in Figure 3, while Table 2 reports the values of total and relative energies for the different stationary points along the two reaction channels.

Starting from these TSs, the related minima associated with the final cycloadducts, **P1** and **P2**, have been obtained. The two possible cycloadditions are very exothermic, in the range of about −43 to −50 kcal/mol (B3LYP/6-31G* results). The greater stability of **P2** relative to **P1** can be attributed to a favorable delocalization of a lone pair of the O1 oxygen atom along the conjugated ester moiety present in **P2**. This delocalization is not possible in **P1**.

The potential energy barrier (PEB) for the more favorable *meta* reaction channel via **TS2** is 10.6 kcal/mol. An analysis of the PEBs for this 1,3-DC shows that the B3LYP/6-31G* calculations predict a neat *meta* regioselectivity, in agreement with experimental results. Thus, the energy of **TS1** is approximately 3.1 kcal/mol higher than that of **TS2**, which thus justifies the preferent formation of **P2**. A comparative analysis of the energy values presented in Table 2 shows that B3LYP/6-31+G* and B3LYP/6-31G* calculations give a similar regioselectivity. Inclusion of diffuse functions increases the PEBs by ca. 3−4 kcal/mol because of both a larger stabilization of **N1** and a decrease of the basis set superposition error at the TSs.[13]

Solvent effects in the activation barriers and selectivity have also been taken into account (Table 2). This leads to an increase of ca. 1 kcal/mol in the PEBs relative to the gas-phase calculations, due to a higher stabilization of the polar nitrone in the liquid phase.[8f,g] These results are in agreement with the small charge-transfer found at the TSs (see later). Moreover, inclusion of solvent effects does not lead to noticeable changes in the regioselectivity, as **TS2** is still predicted to have an energy 2.7 kcal/mol lower than that of **TS1**.

(b) Geometrical Parameters and Analysis of Frequencies. Comparison of the geometrical parameters obtained at the B3LYP/6-31G* and B3LYP/6-31+G* levels shows that there are no significant geometrical differences (Figure 3). For the *ortho* **TS1**, the O1−C2 forming bond is longer than the C3−C4 bond. The difference between the lengths of both forming bonds, $\Delta r_0 = d(\mathrm{O1-C2}) - d(\mathrm{C3-C4})$, is 0.3 Å. The *meta* **TS2** is less symmetric than **TS1**; the difference in lengths of the two bonds being formed, $\Delta r_m = d(\mathrm{C2-C4}) - d(\mathrm{O1-C3})$, is 0.7 Å. In **TS2** the forming O1−C3 bond is shorter than the C2−C4 bond. For these 1,3-DCs, however, the value of Δr cannot be taken as a measure of the asynchronicity of the process, since C−O bonds are shorter than C−C bonds.

The H3−C3−C2 and C3−C4−C10 bond angles are 144° and 171° at **TS1**, and 148° and 164° at **TS2**, respectively. These bond angles indicate the change of hybridization on the C2 and C3 acetylenic centers throughout the cycloaddition process (from sp to sp^2). Moreover, the circumstance that the H3−C3−C2 bond angles are smaller than the C3−C4−C10 bond angles at both TSs is in agreement with the greater extent of bond formation at the β position in the methoxycarbonyl-substituted dipolarophile.

The presence of the electron-withdrawing CO_2Me group in the dipolarophile increases the lack of symmetry of the two bonds being formed in the TSs. The bond in the α position to the CO_2Me group is longer than the bond in position β. For this dipolarophile, the β carbon is more electrophilic than the α carbon. Consequently, there is a stronger degree of bond formation and a shorter bond length at the β carbon in the TSs.

The transition vectors (TVs)[14] for the two aforementioned TSs have similar components. For **TS1**, the dominant TV components are associated with the C3−C4 and O1−C2 bond distances, which correspond to the two single bonds being formed along this 1,3-DC. The value of the C3−C4 component (0.8) is greater than that for the O1−C2 component (0.4). The component associated with the C4−N5 bond length also has a small participation, which indicates the change toward a single bond. Several bond and dihedral angles participate in this TV, which indicates the hybridization changes developing at C3 and N5 (from sp^2 to sp^3). For **TS2**, the dominant TV components are associated with the O1−C3 and C2−C4 bond distances, which correspond to the two single bonds being formed. At these TSs, the TV components have more similar values (0.7 and 0.5, respectively). As in **TS1**, several bond and dihedral angles participate in the TV.

The imaginary frequency value for **TS1** (394i cm^{-1}) is slightly greater than that for **TS2** (388i cm^{-1}). These low values indicate that the processes are associated with the movements of heavy atoms.

(12) Domingo, L. R. *Theor. Chem. Acc.* **2000**, *104*, 240−246.
(13) Domingo, L. R. *J. Org. Chem.* **1999**, *64*, 3922−3929.
(14) McIver, J. W. J.; Komornicki, A. *J. Am. Chem. Soc.* **1972**, *94*, 2625−2633.

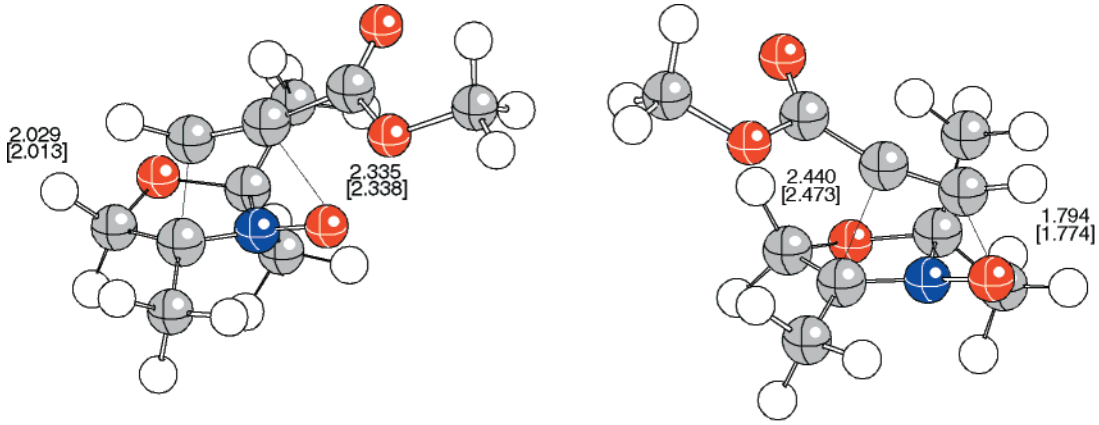

Figure 3. Selected geometrical parameters for transition structures corresponding to the 1,3-DC of nitrone **N1** to methyl propiolate. The values of the lengths of bonds directly involved in the reaction (calculated at the B3LYP/6-31G* and B3LYP/6-31+G* levels [in brackets]) are given in angstroms.

Table 2. Total Energies (au) and Relative Energies[a] (kcal/mol, in parentheses) for the Stationary Points of the 1,3-DCs of Nitrone Model N1 to Methyl Propiolate (MP) or Acrylonitrile (CN)

	B3LYP/6-31G*		B3LYP/6-31+G*		B3LYP/6-31G* (in toluene)	
N1	−440.3965635		−440.415402		−440.399092	
CN	−170.8290724		−170.840302		−170.833987	
MP	−305.200924		−305.216830		−305.202858	
TS1	−745.575580	(13.7)	−745.605624	(16.7)	−745.579103	(14.3)
TS2	−745.580599	(10.6)	−745.609670	(14.2)	−745.583390	(11.6)
P1	−745.665595	(−42.7)	−745.693012	(−38.1)	−745.668689	(−41.9)
P2	−745.677305	(−50.1)	−745.703872	(−45.0)	−745.679565	(−48.7)
TS3-en	−611.201801	(15.0)	−611.224142	(19.8)	−611.206621	(16.6)
TS3-ex	−611.203034	(14.2)	−611.226015	(18.6)	−611.207752	(15.9)
TS4-en	−611.203410	(13.9)	−611.225838	(18.7)	−611.207510	(16.0)
TS4-ex	−611.202202	(14.7)	−611.225128	(19.2)	−611.206599	(16.6)
P3-en	−611.250795	(−15.8)	−611.270831	(−9.5)	−611.255034	(−13.8)
P3-ex	−611.251397	(−16.2)	−611.272503	(−10.5)	−611.255379	(−14.0)
P4-en	−611.254348	(−18.0)	−611.275019	(−12.1)	−611.257767	(−15.5)
P4-ex	−611.251486	(−16.2)	−611.272190	(−10.3)	−611.255568	(−14.1)

[a] Relative to **N1**+**CN** or **N1**+**MP**.

Table 3. Wiberg Bond Orders at Transition Structures TS1, TS2, TS3-en, TS3-ex, TS4-en, and TS4-ex

ortho TSs	**TS1**	**TS3-en**	**TS3-ex**	*meta* TSs	**TS2**	**TS4-en**	**TS4-ex**
O1−C2	0.23	0.27	0.29	O1−C3	0.49	0.53	0.50
C2−C3	2.44	1.44	1.43	C2−C3	2.33	1.35	1.37
C3−C4	0.42	0.48	0.48	C4−C2	0.22	0.32	0.32
C4−N5	1.25	1.22	1.22	C4−N5	1.39	1.33	1.32
O1−N5	1.30	1.30	1.29	O1−N5	1.14	1.14	1.15

(c) Bond Order and Charge Analysis. A more-balanced measure of the extent of bond formation or bond breaking along a reaction pathway is provided by the concept of bond order (BO).[15] This theoretical tool has previously been used to study the molecular mechanism of chemical reactions.[16] To understand the nature of these processes in the case of our substrates, the Wiberg bond indices[11] have been computed by using the natural bond orbital (NBO) analysis[15] as implemented in Gaussian98. The results are included in Table 3.

Analysis of the BOs for these TSs allows for the study of the asynchronicity for the bond formation processes along the two reaction channels (Table 3). For **TS1**, the BO for the forming C3−C4 bond (0.42) has a greater value than that for the forming O1−C2 bond (0.22). For **TS2**, however, the BO for the forming C2−C4 bond (0.22) has a lesser value than that for the forming O1−C3 bond (0.49). These data show a change of the asynchronicity on the bond formation process for the two regioisomeric pathways. The change is controlled by the nonsymmetric dipolarophile, for which the β carbon is more electrophilic than the α carbon. Moreover, the more favorable **TS2** is slightly more asynchronous than **TS1**. This fact is in agreement with the empirical rule which holds for a variety of related cycloadditions that "for dissymetrically substituted dienophiles or dipolarophiles, the more asynchronous process has the lower energy".[13,17] A comparative study of the BOs and frequency analysis also corroborates the observation that the more asynchronous TS presents the lower imaginary frequency.[13]

The natural population analysis for these TSs predicts a small charge transfer, which is only slightly greater for **TS2** (0.12 e) than for **TS1** (0.11 e). This low charge transfer may be due to the presence of the electronegative O1 oxygen atom in the dipole system, which prevents a substantial charge transfer from the dipole to the dipolarophile along the cycloaddition process.

(15) (a) Reed, A. E.; Weinstock, R. B.; Weinhold, F. *J. Chem. Phys.* **1985**, *83*, 735−735. (b) Reed, A. E.; Curtiss, L. A.; Weinhold, F. *Chem.Rev.* **1988**, *88*, 899−926.

(16) (a) Lendvay, G. *J. Phys. Chem.* **1989**, *93*, 4422−4429. (b) Lendvay, G. *J. Phys. Chem.* **1994**, *98*, 6098−6104.

(17) (a) Jorgensen, W. L.; Lim, D.; Blake, J. F. *J. Am. Chem. Soc.* **1993**, *115*, 2936−2942. (b) Froese, R. D. J.; Organ, M. G.; Goddard, J. D.; Stack, T. D. P.; Trost, B. M. *J. Am. Chem. Soc.* **1995**, *117*, 10931−10938.

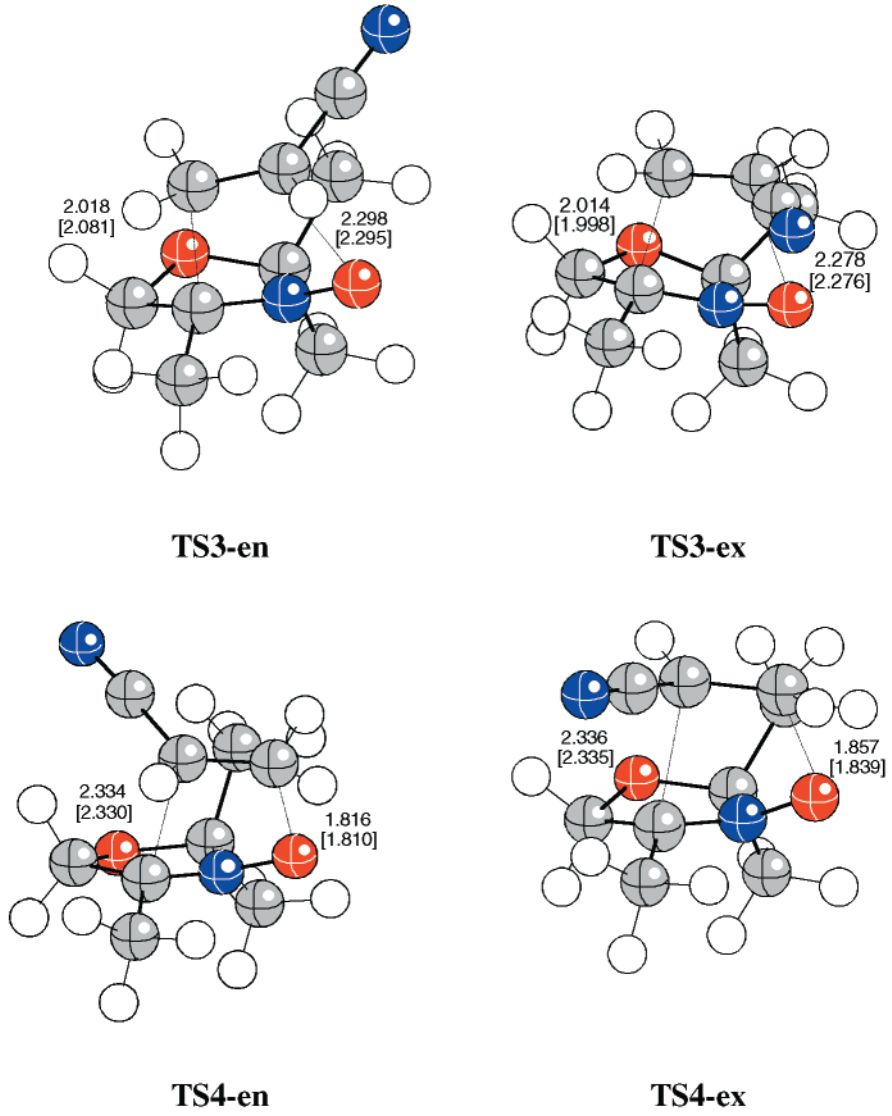

Figure 4. Selected geometrical parameters for transition structures corresponding to the 1,3-DC of nitrone **N1** to acrylonitrile. The values of the lengths of bonds directly involved in the reaction (calculated at the B3LYP/6-31G* and B3LYP/6-31+G* levels [in brackets]) are given in ångstroms.

4. 1,3-DC of N1 to Acrylonitrile. (a) Energies. Four reaction channels corresponding to the *endo* and *exo* approaches of acrylonitrile (dipolarophile) to **N1** (dipole) on the two regioisomeric pathways, *ortho* and *meta*, have been considered (Scheme 7). The stereoisomeric channels along the *ortho* pathways correspond to the O1−C2 and C3−C4 bond-forming processes, whereas the *meta* pathways correspond to the O1−C3 and C2−C4 bond-forming processes. We have thus considered four TSs: **TS3-en**, **TS3-ex**, **TS4-en**, and **TS4-ex**, which correspond to the *endo* and *exo* approach of the polarophile to the dipole along the *ortho* and *meta* pathways, respectively. A schematic representation of the stationary points along the *endo*/*exo* attacks of acrylonitrile to **N1** in the two regioisomeric pathways is presented in Scheme 7, together with the atom numbering.

The geometries of the TSs are displayed in Figure 4. Table 1 reports the values of total and relative energies for the different stationary points along the four reaction channels.

From these TSs, the related minima associated with the final cycloadducts, **P3-en**, **P3-ex**, **P4-en**, and **P4-ex**, have been obtained. **P3** and **P4** are two pairs of diastereomeric cycloadducts. All four possible cycloadditions are exothermic, with the predicted values in the range of −16 to −18 kcal/mol.

B3LYP/6-31G* calculations give a PEB value for the more favorable reaction channel via **TS4-en** of 13.9 kcal/mol. The two regioisomeric *ortho* and *meta* pathways each present a different *endo*/*exo* stereoselectivity. Along the *ortho* pathway, the *exo* approach is favored in relation to the *endo* approach, with **TS3-en** having an energy 0.8 kcal/mol higher than that of **TS3-ex**. The reverse, however, is true for the *meta* pathway, with **TS4-en** having an energy 0.8 kcal/mol lower than that of **TS4-ex**. The *exo* stereoselectivity found along the *ortho* pathway can be explained by a steric hindrance that progressively develops in **TS3-en** between the nitrile group and one of the methyl groups at C6 (Figure 4). On the other hand, the *endo* stereoselectivity predicted for the *meta* pathway, which was not observed experimentally, is explained by a hyperconjugative delocalization in **TS4-en** between the CN group and the neighboring H8 hydrogen atom (2.759 Å). This leads to a stabilization of this TS relative to **TS4-ex**. It is worth mentioning that the experimentally observed *endo* stereoselectivity in the

1,3-DC of an azomethine ylide to acrylonitrile[18] has recently been explained theoretically by invoking this type of hyperconjugative delocalization.[13]

An analysis of the relative energies presented in Table 2 indicates that B3LYP calculations do not clearly predict the regioselectivity of this 1,3-DC. Thus, while B3LYP/6-31G* calculations predict that the *meta* reaction channel via **TS4-en** will be slightly more favorable than the *ortho* channel via **TS3-ex**, B3LYP/6-31+G* calculations suggest the opposite. This inability to predict the regioselectivity of 1,3-DCs reliably has also come up in the study of other related reactions[8f] and can be explained by the FMO analysis for nitrone **N1**, which exhibits similar HOMO coefficient values at the O1 and C4 centers.

Comparative study of the relative energies of the TSs at different computational levels makes clear that regioselectivity predictions are highly dependent on the computational level used (see Supporting Information). As a matter of fact, whereas HF calculations distinctly predict a *meta* regioselectivity in disagreement with experimental results, inclusion of electron correlation and the use of a larger basis set predicts the *ortho* regioselectivity as that favored. Moreover, all computational levels predict an *exo* stereoselectivity for the *ortho* pathway.

As in the reaction with methyl propiolate (see above), inclusion of solvent effects gives rise to an increase of ca. 1.5 kcal/mol in the PEBs relative to gas-phase calculations (Table 2). Once again, the reason is the appreciable stabilization of the polar nitrone in the liquid phase.[8f,g] One aspect is worth mentioning here. When solvent effects are included, the *ortho* pathway is predicted to be slightly more favorable than the *meta* pathway. In the absence of solvent, however, the contrary is true. These results are in agreement with those for related 1,3-DCs of nitrones found by Cossío et al.,[8f] who stated that the regioselectivity could not be predicted with the aid of simple electronic arguments, and that the polarization of the solute had to be taken into account.

(b) Geometrical Parameters and Analysis of Frequencies. A comparison of the geometrical parameters obtained at the B3LYP/6-31G* and B3LYP/6-31+G* levels shows that there are no significant geometrical differences (Figure 4). For the regioisomeric *ortho* pathways, the O1−C2 forming bonds are longer at the TSs than the C3−C4 bonds. The differences in length between both forming bonds, $\Delta r_0 = d(\mathrm{O1-C2}) - d(\mathrm{C3-C4})$ are about 0.3 Å and are thus slightly greater for **TS3-en** than for **TS3-ex**. This is due to the steric hindrance that progressively develops along the *endo* approach, with a subsequent increase of the O1−C2 distance.

In *meta* pathways, the TSs are still less symmetric than in *ortho* pathways; the length differences of the two forming bonds, $\Delta r_m = d(\mathrm{C2-C4}) - d(\mathrm{O1-C3})$ are approximately 0.4 Å. In these TSs, the O1−C3 forming bonds are shorter than the C2−C4 bonds; moreover, the O1−C3 bond in **TS4-en** is slightly shorter than in **TS4-ex**. Again, this is due to the favorable hyperconjugative interaction that progressively develops along the *endo* TS and which increases the asynchronicity of the process.[13]

The presence of the electron-withdrawing C≡N group in the dipolarophile increases the lack of symmetry of the two bonds being formed in these TSs. The bond in position α to the nitrile group is longer than that in *β* position; for this dipolarophile, the *β* carbon is more electrophilic than the α carbon. Consequently, there is a stronger degree of bond formation and a shorter bond length at the *β* carbons in these TSs.

The TVs for the four aforementioned TSs have similar components. For the *ortho* TSs, the dominant TV components are associated with the C3−C4 and O1−C2 bond distances, which correspond to the two single bonds being formed along these 1,3-DC reactions. The values for the C3−C4 component (0.8) are larger than those for the O1−C2 component (0.4). In these TSs, the component associated with the C4−N5 bond length also has a small participation, which indicates the change toward a single bond. Several bond and dihedral angles participate in these TVs, a fact which points to the hybridization changes developing at C3 and N5 (from sp^2 to sp^3). For *meta* TSs, the dominant TV components are associated with the O1−C3 and C2−C4 bond distances, which correspond to the two single bonds being formed; these components have similar values (approximately 0.6). Like the *ortho* TSs, the fact that several bond and dihedral angles participate in the TV indicates the hybridization changes developing at C3 and N5 (from sp^2 to sp^3).

The imaginary frequency values for **TS3-en** and **TS3-ex** (407i and 413i cm^{-1}, respectively) are slightly lower than those for **TS4-en** and **TS4-ex** (421i and 427i cm^{-1}, respectively). Again, these low values indicate that these processes are associated with motions of heavy atoms.

(c) Bond Order and Charge Analysis. Analysis of the BOs for these TSs allows for the study of the asynchronicity for the bond formation processes along the four reaction channels. For the *ortho* pathways, the BOs for the bonds forming at C3−C4 (0.48 for **TS3-en** and **TS3-ex**) have higher values than for the O1−C2 bonds (0.27 and 0.29 for **TS3-en** and **TS3-ex**, respectively). In the *meta* pathways, however, the BOs for the bonds forming at C2−C4 (0.32 for **TS4-en** and **TS4-ex**) have lesser values than for the O1−C3 bonds (0.53 and 0.50 for **TS4-en** and **TS4-ex**, respectively). As was the case for the reaction with methyl propiolate, these data show a change of the asynchronicity for the two regioisomeric pathways. The change is controlled by the nonsymmetric dipolarophile, in which the *β* carbon is more electrophilic than the α carbon. For acrylonitrile, the *ortho* TSs are slightly more asynchronous than the *meta* TSs. Furthermore, a comparative study of the BOs and frequency analysis indicates that the more asynchronous TS has the lower imaginary frequency.[13]

The natural population analysis for these TSs predicts a small charge transfer (about 0.1 e). As in the reaction with methyl propiolate, this low charge transfer is likely related to the presence of the electronegative O1 oxygen atom in dipole **N1**, which prevents a substantial charge transfer toward the dipolarophile.

Concluding Remarks

We have investigated 1,3-DCs of the chiral nitrone **1** to several dipolarophiles. The final purpose was to be able to use the cycloadducts in the synthesis of various types of chiral, nitrogenated compounds such as nonproteinogenic amino acids, amino alcohols, amino sugars, etc. From all of these cycloadditions, that with acrylonitrile displayed a complete regioselectivitiy, as well as a

(18) Laduron, F.; Ates, C.; Viehe, H. G. *Tetrahedron Lett.* **1996**, *37*, 5515−5518.

marked stereoselectivity, which makes the process attractive for the mentioned synthetic purposes.

We have used B3LYP calculations with the 6-31G* and 6-31+G* basis sets for the study of the mechanism of the 1,3-DCs of a reduced nitrone model **N1** to both methyl propiolate and acrylonitrile. The different reaction pathways have been mapped out, and the reactants, TSs, and cycloadducts have been located and properly characterized. Relative rates, regioselectivity, and *endo*/*exo* stereoselectivity have been analyzed and discussed as a function of the substituents on the dipolarophiles. These ab initio methods predict one-step cycloaddition processes via asynchronous transition structures. For the 1,3-DC with methyl propiolate, calculations at these levels suggest a neat *meta* regioselectivity, in agreement with experimental results. For the 1,3-DC with acrylonitrile, the predicted regioselectivity proves to be dependent on the computational level; in fact, electron correlation and diffuse functions have to be included in order to explain the experimentally observed *ortho* regioselectivity. Furthermore, the reaction displays an *exo* stereoselectivity; the *endo* approach is disfavored because of a steric hindrance that appears between the CN group in the dipolarophile and a proximal methyl group at C6 in the dipole.

Experimental Section

General. NMR spectra were measured at 22 °C. The signals of the deuterated solvent ($CDCl_3$) were taken as the reference. Unambiguous assignments of signals were made with a combination of spin decoupling, DEPT, and HMQC experiments. High-resolution mass spectra were run either by the electron impact (EIMS, 70 eV), chemical ionization (CIMS, CH_4), or fast atom bombardment mode (FABMS, *m*-nitrobenzyl alcohol matrix). Samples for IR spectral measurements were prepared as oily films on NaCl plates (oils) or KBr pellets (solids). Optical rotations were measured at 22 °C. Column chromatography (CC) was performed on silica gel Süd-Chemie AG (50−200 μm) with the solvent mixture indicated in each case. Toluene was freshly distilled from sodium wire and was transferred via syringe. Commercially available reagents (Aldrich or Fluka) were used as received.

Computing Methods. In recent years, theoretical methods based on the DFT[19] have emerged as an alternative to traditional ab initio methods in the study of structure and reactivity of chemical systems. Density functional studies on Diels−Alder and related reactions have shown that functionals including gradient corrections and hybrid functionals, such as B3LYP,[20] together with the 6-31G* basis set,[21] give PEBs in good agreement with experimental results.[22] Recently, several DFT studies devoted to 1,3-DCs carried out with the B3LYP functionals, together with the 6-31G* and 6-31+G* basis sets, have shown that this computational level also yields accurate PEBs for this type of cycloadditions.[8c−g] We have therefore carried out geometrical optimizations with the aid of the gradient corrected functional of Becke, Lee, Yang, and Parr (B3LYP) for exchange and correlation, together with the standard 6-31G* basis set. The stationary points were characterized by frequency calculations in order to verify that minima and transition structures have zero and one imaginary frequency, respectively. The optimizations were carried out using the Berny analytical gradient optimization method.[23] The transition vector,[14] i.e., the eigenvector associated with the unique negative eigenvalue of the force constants matrix, has been characterized. Since it was expected that some negative charge may be located in some stationary points, the 6-31+G* basis set[21] was also used because of its superior ability to accommodate negative charges. All calculations were carried out with the Gaussian 98 suite of programs.[24] Optimized geometries of all the structures are available from one of the authors (L.R.D.). The electronic structures of stationary points were analyzed by the NBO method.[15]

Solvent effects on these 1,3-DC reactions were considered by means of B3LYP/6-31G* single point calculations at the gas phase stationary points. A relatively simple self-consistent reaction field (SCRF)[25] method based on the polarizable continuum model (PCM) of Tomasi's group[26] was used for this purpose. In this procedure, the solvent, which is characterized by its dielectric constant (ϵ), is assimilated into a continuous medium, which surrounds a molecular-shaped cavity in which the solute is placed. In the experimental work described here, toluene (dielectric constant, $\epsilon = 2.24$) was used as the solvent in most cases.

(*R*)-4-(2,2-Dimethyl-1,3-dioxolan-4-yl)-2,2-dimethyl-2,5-dihydro-1,3-oxazole *N*-oxide, (1) and (*R*)-3-(2,2-Dimethyl-1,3-dioxolan-4-yl)-6,6-dimethyl-4*H*-1,5,2-dioxazine (2). Erythrulose 3,4-acetonide[27] (8 g, ca. 50 mmol) was dissolved in dry MeOH (125 mL) and treated with hydroxylamine hydrochloride (3.50 g, ca. 50 mmol) and NaOAc (8.20 g, ca. 100 mmol). After stirring for 2 h at room temp, the creamy reaction mixture was diluted with CH_2Cl_2 (25 mL) and treated with small portions of solid Na_2CO_3 (until bubbling of CO_2 ceases). The mixture was then filtered through Celite and evaporated in vacuo. Column chromatography of the residue on silica gel (hexanes−EtOAc 1:1) afforded erythrulose 3,4-acetonide oxime as a mixture of syn/anti stereoisomers (7.33 g).

The oxime mixture obtained above and *p*-toluenesulfonic acid (170 mg, ca. 1 mmol) were dissolved in a 4:1 mixture of acetone and 2,2-dimethoxypropane (150 mL). The resulting mixture was stirred at room temp for 18 h. After solvent removal in vacuo, the oily residue was chromatographed on silica gel (hexanes−EtOAc 7:3) to yield, first dioxazine **2** (3.23 g, 30% overall from erythrulose acetonide) and then nitrone **1** (2.80 g, 26% overall from erythrulose acetonide).

(19) (a) Parr, R. G.; Yang, W. *Density Functional Theory of Atoms and Molecules*; Oxford University Press: New York, 1989. (b) Ziegler, T. *Chem. Rev.* **1991**, *91*, 651−667.

(20) (a) Lee, C.; Yang, W.; Parr, R. G. *Phys. Rev. B* **1988**, *37*, 785−789. (b) Becke, A. D. *J. Chem. Phys.* **1993**, *98*, 5648−5652.

(21) Hehre, W. J.; Radom, L.; Schleyer, P. von R.; Pople, J. A. *Ab initio Molecular Orbital Theory*; Wiley: New York, 1986.

(22) (a) Goldstein, E.; Beno, B.; Houk, K. N. *J. Am. Chem. Soc.* **1996**, *118*, 6036−6043. (b) Sbai, A.; Branchadell, V.; Ortuño, R. M.; Oliva, A. *J. Org. Chem.* **1997**, *62*, 3049−3054. (c) Branchadell, V.; Font, J.; Moglioni, A. G.; Ochoa de Echaguen, C.; Oliva, A.; Ortuño, R. M.; Veciana, J.; Vidal Gancedo, J. *J. Am. Chem. Soc.* **1997**, *119*, 9992−10003. (d) García, J. I.; Martínez-Merino, V.; Mayoral, J. A.; Salvatella, L. *J. Am. Chem. Soc.* **1998**, *120*, 2415−2420. (e) Domingo, L. R.; Arnó, M.; Andrés, J. *J. Am. Chem. Soc.* **1998**, *120*, 1617−1618. (f) Domingo, L. R.; Picher, M. T.; Zaragozá, R. J. *J. Org. Chem.* **1998**, *63*, 9183−9189. (g) Tietze, L. F., Pfeiffer, T., Schuffenhauer, A. *Eur. J. Org. Chem.* **1998**, 2773−2741.

(23) Schlegel, H. B. Geometry Optimization on Potential Energy Surface. In *Modern Electronic Structure Theory*; Yarkony, D. R., Ed.; World Scientific Publishing: Singapore, 1994.

(24) Frisch, M. J.; Trucks, G. W.; Schlegel, H. B.; Scuseris, G. E.; Robb, M. A.; Cheeseman, J. R.; Zakrezewski, V. G.; Montgomery, J. A.; Stratmann, R. E.; Burant, J. C.; Dapprich, S.; Millam, J. M.; Daniels, A. D.; Kudin, K. N.; Strain, M. C.; Farkas, O.; Tomasi, J.; Barone, V.; Cossi, M.; Cammi, R.; Mennucci, B.; Pomelli, C.; Adamo, C.; Clifford, S.; Ochterski, J.; Peterson, G. A.; Ayala, P. Y.; Cui, Q.; Morokuma, K.; Malick, D. K.; Rabuck, A. D.; Raghavachari, K.; Foresman, J. B.; Cioslowski, J.; Ortiz, J. V.; Stefanov, B. B.; Liu, G.; Liashenko, A.; Piskorz, P.; Komaromi, R.; Gomperts, R.; Martin, R. L.; Fox, D. J.; Keith, T.; Al-Laham, M. A.; Peng, C. Y.; Nanayakkara, A.; González, C.; Challacombe, M.; Gill, P. M. W.; Johnson, B. G.; Chen, W.; Wong, M. W.; Andres, J. L.; Head-Gordon, M.; Replogle, E. S.; Pople, J. A., *Gaussian 98* (Revision A.1); Gaussian, Inc., Pittsburgh, PA, 1998.

(25) (a) Tomasi, J.; Persico, M. *Chem. Rev.* **1994**, *94*, 2027−2094. (b) Simkin, B. Y.; Sheikhet, I. *Quantum Chemical and Statistical Theory of Solutions-A Computational Approach*; Ellis Horwood: London, 1995.

(26) (a) Cances, M. T.; Mennunci, V.; Tomasi, J. *J. Chem. Phys.* **1997**, 107, 3032−3041. (b) Cossi, M.; Barone, V.; Cammi, R.; Tomasi, *J. Chem. Phys. Lett.* **1996**, 255, 327−335. (c) Barone, V.; Cossi, M.; Tomasi, J. *J. Comput. Chem.* **1998**, *19*, 404−417.

(27) Carda, M.; Rodríguez, S.; Murga, J.; Falomir, E.; Marco, J. A.; Röper, H. *Synth. Commun.* **1999**, *29*, 2601−2610.

(1): Colorless needles, mp 56−57° (from hexane−CH_2Cl_2), $[\alpha]^{22}_D$ −1.8 (*c* 1.3, $CHCl_3$); ^{1}H NMR (400 MHz) δ 5.21 (ddd, 7, 5.5, 1.5 Hz, 1H, H-4′), 4.85 (dd, 15, 1.5 Hz, 1H, H-5$_a$), 4.75 (dd, 15, 1.5 Hz, 1H, H-5$_b$), 4.37 (dd, 9, 7 Hz, 1H, H-5′$_a$), 3.93 (dd, 9, 5.5 Hz, 1H, H-5′$_b$), 1.54, 1.53, 1.39, 1.34 (4 × s, 4 × 3H, acetonide Me); ^{13}C NMR (100 MHz) δ 137.7 (C-4), 110.3 (C-2′), 106.1 (C-2), 69.9 (C-4′), 67.9 (C-5), 67.1 (C-5′), 26.0, 24.6, 24.4, 24.0 (acetonide Me); IR ν_{max} 1615 (C═N) cm^{-1}; HRCIMS *m*/*z* (% rel inten) 216.1231 [M + H$^+$]. Calcd for $C_{10}H_{18}NO_4$, 216.1236. Anal. Calcd for $C_{10}H_{17}NO_4$: C, 55.80; H, 7.96; N, 6.51. Found, C, 55.90; H, 8.00; N, 6.32.

(2): Colorless needles, mp 45−46° (from hexane−CH_2Cl_2); $[\alpha]^{22}_D$ +4.9 (*c* 2.1, $CHCl_3$); ^{1}H NMR (400 MHz) δ 4.69 (dd, 7, 6 Hz, 1H, H-4′), 4.29, 4.24 (AB system, 18 Hz, 2H, H-4$_a$/H-4$_b$), 4.19 (dd, 8.8, 7 Hz, 1H, H-5′$_a$), 4.03 (dd, 8.8, 6 Hz, 1H, H-5′$_b$), 1.43, 1.42, 1.41, 1.35 (4 × s, 4 × 3H, acetonide Me); ^{13}C NMR (100 MHz) δ 156.6 (C-3), 110.3 (C-2′), 98.3 (C-6), 75.1 (C-4′), 67.0 (C-5′), 55.8 (C-4), 26.0, 24.7, 23.4, 23.0 (acetonide Me); IR ν_{max} 1634 (C═N) cm^{-1}; HRCIMS *m*/*z* (% rel inten) 216.1237 [M + H$^+$]. Calcd for $C_{10}H_{18}NO_4$, 216.1236. Anal. Calcd for $C_{10}H_{17}NO_4$: C, 55.80; H, 7.96; N, 6.51. Found, C, 56.00; H, 7.84; N, 6.40.

General Experimental Procedure for Dipolar Cycloadditions of Nitrone 1. Nitrone **1** (1 mmol) and the appropriate dipolarophile (1.1 mmol) were dissolved in dry toluene (6 mL) and heated at reflux under argon for 2 h. The reactions with volatile dipolarophiles (cyclohexene, 2,3-dimethyl-2-butene, ethyl vinyl ether) were conducted at 150 °C (external temperature) in a closed system under pressure, with the dipolarophile as the solvent. In all cases, the solvent was then removed, and the oily residue was chromatographed on silica gel (hexanes−EtOAc 4:1). Overall yields and proportions of diastereoisomers are indicated in Table 1.

Dimethyl (3a*S*)-3a-[(4*R*)-2,2-Dimethyl-1,3-dioxolan-4-yl]-6,6-dimethyl-3a,4-dihydro[1,3]oxazolo[3,4-*b*]isoxazole-2,3-dicarboxylate (3): colorless cubes, mp 83−84 °C (from hexanes−Et_2O); $[\alpha]^{22}_D$ +54.5 (*c* 0.32, $CHCl_3$); ^{1}H NMR (400 MHz) δ 4.58 (t, 7 Hz, 1H, H-4′), 4.24 (d, 9.3 Hz, 1H, H-4$_a$), 4.07 (d, 9.3 Hz, 1H, H-4$_b$), 4.01 (dd, 8.2, 7 Hz, 1H, H-5′$_a$), 3.92 (dd, 8.2, 7 Hz, 1H, H-5′$_b$), 3.88, 3.71 (2 × s, 2 × 3H, OMe), 1.51, 1.41, 1.40, 1.36 (4 × s, 4 × 3H, acetonide Me); ^{13}C NMR (100 MHz) δ 162.2, 158.9 (ester C═O), 154.4 (C-2), 110.2 (C-2'), 105.5 (C-3), 103.4 (C-6), 81.0 (C-3a), 74.2 (C-4′), 68.8 (C-4), 66.2 (C-5′), 53.4, 52.0 (2 × OMe), 25.9, 25.7, 24.2, 22.9 (acetonide Me); IR ν_{max} 1756, 1712 (C═O) cm^{-1}; HREIMS *m*/*z* (% rel inten) 357.1422 [M]$^+$. Calcd for $C_{16}H_{23}NO_8$, 357.1423. Anal. Calcd for $C_{16}H_{23}NO_8$: C, 53.78; H, 6.49; N, 3.92. Found, C, 54.00; H, 6.66; N, 4.01.

Dimethyl (3a*R*)-3a-[(4*R*)-2,2-dimethyl-1,3-dioxolan-4-yl]-6,6-dimethyl-3a,4-dihydro [1,3]oxazolo[3,4-b]isoxazole-2,3-dicarboxylate (4): oil; $[\alpha]^{22}_D$ −74 (*c* 1, $CHCl_3$); ^{1}H NMR (400 MHz) δ 4.50 (d, 9.9 Hz, 1H, H-4$_a$), 4.35 (t, 7 Hz, 1H, H-4′), 4.06 (dd, 8.7, 7 Hz, 1H, H-5′$_a$), 3.92 (d, 9.9 Hz, 1H, H-4$_b$), 3.88 (dd, 8.7, 7 Hz, 1H, H-5′$_b$), 3.86, 3.72 (2 × s, 2 × 3H, OMe), 1.46, 1.38, 1.37, 1.33 (4 × s, 4 × 3H, acetonide Me); ^{13}C NMR (100 MHz) δ 162.5, 158.6 (ester C═O), 152.7 (C-2), 109.7 (C-2'), 107.1 (C-3), 103.1 (C-6), 80.9 (C-3a), 78.1 (C-4′), 69.3 (C-4), 65.9 (C-5′), 53.3, 52.0 (2 × OMe), 25.8, 25.1, 24.8, 22.0 (acetonide Me); IR ν_{max} 1754, 1716 (C═O) cm^{-1}; HREIMS *m*/*z* (% rel inten) 357.1429 [M]$^+$. Calcd for $C_{16}H_{23}NO_8$, 357.1423.

Ethyl (3a*S*)-3a-[(4*R*)-2,2-dimethyl-1,3-dioxolan-4-yl]-6,6-dimethyl-3a,4-dihydro[1,3] oxazolo[3,4-b]isoxazole-3-carboxylate (6): colorless plates, mp 59−60 °C (from hexanes−Et_2O); $[\alpha]^{22}_D$ +73.5 (*c* 0.53, $CHCl_3$); ^{1}H NMR (400 MHz) δ 7.40 (s, 1H, H-2), 4.66 (dd, 7.5, 6.8 Hz, 1H, H-4′), 4.18 (d, 9 Hz, 1H, H-4$_a$), 4.16 (q, 7 Hz, 3H, OC*H*$_2$CH$_3$), 4.06 (d, 9 Hz, 1H, H-4$_b$), 3.97 (dd, 8, 6.8 Hz, 1H, H-5′$_a$), 3.88 (dd, 8, 7.5 Hz, 1H, H-5′$_b$), 1.50, 1.42, 1.41, 1.36 (4 x s, 4 × 3H, acetonide Me), 1.26 (t, 7 Hz, 3H, OCH$_2$C*H*$_3$); ^{13}C NMR (100 MHz) δ 163.1 (ester C═O), 154.4 (C-2), 110.2 (C-2'), 107.4 (C-3), 103.0 (C-6), 79.3 (C-3a), 74.1 (C-4′), 68.8 (C-4), 66.4 (C-5′), 60.3 (O*C*H$_2$CH$_3$), 26.0, 25.7, 24.2, 23.1 (acetonide Me), 14.3 (OCH$_2$*C*H$_3$); IR ν_{max} 1702 (C═O) cm^{-1}; HRFABMS *m*/*z* 314.1605 [M + H$^+$]. Calcd for $C_{15}H_{24}NO_6$, 314.1603. Anal. Calcd for $C_{15}H_{23}NO_6$: C, 57.50; H, 7.40; N, 4.47. Found, C, 57.70; H, 7.61; N, 4.61.

Ethyl (3a*R*)-3a-[(4*R*)-2,2-dimethyl-1,3-dioxolan-4-yl]-6,6-dimethyl-3a,4-dihydro[1,3]oxazolo[3,4-*b*]isoxazole-3-carboxylate (7): oil; $[\alpha]^{22}_D$ −87 (*c* 1.5, $CHCl_3$); ^{1}H NMR (400 MHz) δ 7.45 (s, 1H, H-2), 4.40 (dd, 7.7, 6.5 Hz, 1H, H-4′), 4.32 (d, 9.3 Hz, 1H, H-4$_a$), 4.16 (q, 7 Hz, 3H, OC*H*$_2$CH$_3$), 4.04 (dd, 8.8, 6.5 Hz, 1H, H-5′$_a$), 3.93 (d, 9.3 Hz, 1H, H-4$_b$), 3.92 (dd, 8.8, 7.7 Hz, 1H, H-5′$_b$), 1.46, 1.42, 1.41, 1.36 (4 × s, 4 × 3H, acetonide Me), 1.26 (t, 7 Hz, 3H, OCH$_2$C*H*$_3$); ^{13}C NMR (100 MHz) δ 163.1 (ester C═O), 155.0 (C-2), 109.3 (C-2′), 107.3 (C-3), 102.7 (C-6), 78.8 (C-3a), 77.8 (C-4′), 67.6 (C-4), 66.2 (C-5′), 60.3 (O*C*H$_2$CH$_3$), 26.0, 25.4, 24.5, 22.6 (acetonide Me), 14.3 (OCH$_2$*C*H$_3$); IR ν_{max} 1706 (C═O) cm^{-1}; HRFABMS *m*/*z* 314.1607 [M + H$^+$]. Calcd for $C_{15}H_{24}NO_6$, 314.1603.

(2*S*,3a*S*)-3a-[(4*R*)-2,2-Dimethyl-1,3-dioxolan-4-yl]-6,6-dimethylperhydro[1,3]oxazolo[3,4-*b*]isoxazole-2-carbonitrile (9): colorless needles, mp 95−96 °C (from hexanes−Et_2O); $[\alpha]^{22}_D$ +46.2 (*c* 3.1, $CHCl_3$); ^{1}H NMR (400 MHz) δ 4.79 (dd, 8, 7 Hz, 1H, H-2), 4.34 (t, 7 Hz, H-4′), 4.12 (dd, 8.5, 7 Hz, 1H, H-5′$_a$), 3.85 (AB system, 10 Hz, 2H, H-4$_a$/4$_b$), 3.77 (dd, 8.5, 7 Hz, 1H, H-5′$_b$), 2.74 (dd, 12.5, 8 Hz, 1H, H-3$_a$), 2.55 (dd, 12.5, 7 Hz, 1H, H-3$_b$), 1.49, 1.47, 1.37, 1.34 (4 × s, 4 × 3H, acetonide *Me*); ^{13}C NMR (100 MHz) δ 116.3 (*C*≡N), 110.4 (C-2′), 102.2 (C-6), 77.0 (C-4′), 76.8 (C-3a), 71.1 (C-4), 66.2 (C-2 + C-5′), 44.1 (C-3), 26.1, 24.8, 24.7, 22.6 (acetonide Me); IR ν_{max} 2306 (C≡N) cm^{-1}; HRCIMS *m*/*z* (% rel inten) 269.1499 [M + H$^+$]. Calcd for $C_{13}H_{21}N_2O_4$, 269.1501. Anal. Calcd for $C_{13}H_{20}N_2O_4$: C, 58.19; H, 7.51; N, 10.44. Found, C, 58.02; H, 7.66; N, 10.65.

(2*R*,3a*R*)-3a-[(4*R*)-2,2-Dimethyl-1,3-dioxolan-4-yl]-6,6-dimethylperhydro[1,3]oxazolo[3,4-*b*]isoxazole-2-carbonitrile (10): colorless needles, mp 83−84 °C (from hexanes−Et_2O); $[\alpha]^{22}_D$ −37.5 (*c* 0.9, $CHCl_3$); ^{1}H NMR (400 MHz) δ 4.70 (dd, 9.6, 6.2 Hz, 1H, H-2), 4.36 (dd, 7, 5.2 Hz, H-4′), 4.15 (dd, 9.3, 7 Hz, 1H, H-5′$_a$), 3.97 (br s, 2H, H-4$_a$/4$_b$), 3.95 (dd, 9.6, 5.2 Hz, 1H, H-5′$_b$), 2.68 (dd, 12.5, 9.6 Hz, 1H, H-3$_a$), 2.55 (dd, 12.5, 6.2 Hz, 1H, H-3$_b$), 1.46, 1.45, 1.33, 1.27 (4 × s, 4 × 3H, acetonide Me); ^{13}C NMR (100 MHz) δ 115.8 (*C*≡N), 110.3 (C-2'), 102.0 (C-6), 79.1 (C-4′), 76.6 (C-3a), 73.9 (C-4), 66.0 (C-5′), 65.9 (C-2), 43.6 (C-3), 26.1, 24.5, 24.2, 22.3 (acetonide Me); IR ν_{max} 2306 (C≡N) cm^{-1}; HRCIMS *m*/*z* (% rel inten) 269.1500 [M + H$^+$]. Calcd for $C_{13}H_{21}N_2O_4$, 269.1501. Anal. Calcd for $C_{13}H_{20}N_2O_4$: C, 58.19; H, 7.51; N, 10.44. Found, C, 58.32; H, 7.46; N, 10.55.

Acknowledgment. Financial support for this project was provided through the Spanish Ministry of Education and Culture (DGICYT projects PB96-0760, PB98-1429, and PB98-1438). All calculations were performed on a Cray-Silicon Graphics Origin 2000 with 64 processors of the Servicio de Informática de la Universidad de Valencia. We are most indebted to this center for providing us with computer capabilities.

Supporting Information Available: One table giving the total and relative energies for the transition structures of the 1,3-DC reaction between nitrone **N1** and acrylonitrile at different computational levels. Two tables giving the imaginary frequencies, Hessian unique negative eigenvalue, main components of the transition vector, and geometric parameters for the transition structures corresponding to the 1,3-DCs between **N1** and methyl propiolate and between **N1** and acrylonitrile. This material is available free of charge via the Internet at http://pubs.acs.org.

JO0009651